Sustainable Chemical Engineering
http://ojs.wiserpub.com/index.php/SCE/

UNIVERSAL WISER PUBLISHER

Research Article

Effect of SrO and ZnO on Densification and in Vitro Behaviors of P_2O_5-CaO-Na_2O-SiO_2-TiO_2 Bioactive Glass-Ceramics

Seyedsahameddin Razavi, Bijan Eftekhari Yekta*, Alireza Khavandi

School of Material science and Engineering, Iran University of science and technology, Tehran, Iran
E-mail: beftekhari@iust.ac.ir

Received: 02 November 2021; **Revised:** 10 January 2022; **Accepted:** 11 January 2022

Abstract: Phosphate based-glass ceramics in the system of P_2O_5-CaO-Na_2O-SiO_2-TiO_2 were obtained by the sintering method. For evaluating the effect of strontium and zinc, different amounts of these elements were doped in the parent glass instead of calcium oxide. Sintering behavior of the glasses was evaluated through the measurement of bulk density, liquid absorption, and open porosity percentages. Based on the results, 600 °C was determined as the optimum sintering temperature. Based on the X-Ray diffractometry, calcium pyrophosphate was precipitated during the sintering process as the main crystallized phase. It is worth noting that changing the parent glass composition led to its phase transformation. Variation in the pH and ion concentration in the simulated body fluid as well as weight loss percentages of the samples were considered to evaluate the dissolution behavior of the samples. The in vitro tests showed that increasing the amount of strontium and zinc intensified the dissolution rate. According to scanning electron micrographs, hydroxyapatite nuclei precipitated on the surfaces of the samples after three days of simulated body fluid (SBF) soaking; but, they were dissolved in the solution after 28 days due to the dissolution of the substrate. Some residues of the grown apatite-like layer were observed on the surface of the composition when 25 and 2.5 molar percent of calcium were substituted for strontium and zinc, respectively.

***Keywords*:** phosphate-based glasses, in vitro behavior, sinterability

1. Introduction

The demand for bone regenerative and repairing materials has exponentially increased by the aging of the world population which leads to prevailing degenerative bone diseases such as osteoporosis.[1] Bioactive glasses have some special properties that make them an ideal choice for this purpose. Their bioactivity can be tailored and their dissolution rate can be controlled to coincide with the growth of new bone.[2] Their ability to form a layer of hydroxyapatite on the specimen's surface provides a coherent interface between the glass surface and body tissues.[3] However, bioactivity can be affected by crystallization which may lead to contradictory results.[4] For example, in both silicate and phosphate based-glasses, it was reported that crystallization can prevent or decelerate the glass bioactivity.[5-8]

Some unique properties of phosphate-based glasses such as their dissolution behavior, which can be dissolved entirely in aqueous solutions, have made them a promising bioactive material for biomedical uses.[9] Their dissolution rate can be controlled by the addition of metal oxides like titanium oxide which can bring about a positive response from

DOI: https://doi.org/10.37256/sce.3120221228

bone cells too.[10] On the other hand, it is highly likely that they will be compatible with the bone as they have common constituent ions.[11] It is known that zinc plays a significant role in the human body. Zinc consumption by metalloenzymes activates different actions like structure, catalytic, or regulatory actions. For example, alkaline phosphatase is one of these enzymes which is essential for ossification.[12] Apart from its antimicrobial role, it was reported that zinc not only can prevent osteoclasts' activities but also motivates osteoblast cells.[13,14] On the other hand, doping zinc in bioactive glasses can enhance calcium phosphate nucleation, due to increasing the surface area while soaking in the SBF solution.[1,2]

Strontium is a divalent cation that is located in the second group of the periodic table as calcium. Protelos®, the trade name of strontium ranelate, is a medicine that has been prescribed for postmenopausal women to prevent osteoporosis and diminish the risk of concomitant fractures.[3,4] Strontium has recently been used for biomedical applications especially in bone tissue engineering.[5-7] It was reported that alkaline phosphatase (ALP) and apatite mineralization activities were enhanced by strontium incorporation into bioactive glasses.[8,9] Novel bioactive glass compositions have been synthesized by strontium and zinc co-doping in silicate-based glasses.[10,11] Boyd et al. suggested that strontium and zinc incorporation into these glasses leads to higher cell viability and biocompatibility.[12] In this context, strontium and zinc were incorporated into a phosphate-based glass system to evaluate their effect on the sintering and crystallization as well as bioactivity and dissolution rate.

2. Materials and characterization methods

2.1 *Samples preparation*

The nominal composition of the primary phosphate-based glass system consisted of 47 P_2O_5, 30.5 CaO, 17.5 Na_2O, and 5 mol ratio TiO_2 in which, for controlling the dissolution behavior 5 mol P_2O_5 was then substituted by SiO_2. For evaluating the effect of strontium and zinc oxides, various parts of CaO were replaced by SrO and ZnO (see Table 1 for glass codes and compositions). Phosphorous pentoxide (P_2O_5), calcium carbonate ($CaCO_3$), sodium carbonate (Na_2CO_3), silicon dioxide (SiO_2), titanium dioxide (TiO_2), strontium nitrate ($Sr(NO_3)_2$), and zinc oxide (ZnO) were used as precursors and all chemicals were above 98% purity and prepared from Merck Co., Germany.

Table 1. Chemical composition of various samples (mol. ratio)

Samples	P_2O_5	CaO	Na_2O	TiO_2	SiO_2	SrO	ZnO
1	47	30.5	17.5	5	0	0	0
2	42	30.5	17.5	5	5	0	0
3	42	27.15	17.5	5	5	3.05	0.305
4	42	22.12	17.5	5	5	7.625	0.76
5	42	13.73	17.5	5	5	15.25	1.52

The batches were prepared as per the compositions given in Table 1 by weighting reactants precisely and mixing them homogeneously. Melt quenching technique was performed to prepare glasses by melting batches in alumina crucibles at 1150 °C for 30 minutes in air at the heating rate of 10 °C/min. Stainless steel rotary rollers were applied to obtain frit by casting the molten mixture between them. Eventually acquired frits were pulverized in agate mortar until to reach powders with particles smaller than 58 μm (mesh no. 270). The crystallinity of the quenched glass and the sintered ones was checked by X-ray diffraction (APOH-8) using Cu-Kα radiation. The diffraction angle was between 5° and 100° while the angular step was 0.1 degrees.

The shaping of the glass powders was performed within a stainless steel cylindrical die, with a 10 mm diameter,

using uniaxial pressing under a pressing load of 134 MPa.

2.2 *Sintering and thermal behavior*

To evaluate the sintering and crystallization behavior of glasses, pellets of each glass were sintered at different temperatures between 570° and 700° for 1 h at a heating rate of 10 °C/min in air and then were freely cooled down to room temperature inside the furnace. This sintering interval temperature was adopted regarding the differential thermal analysis result of the initial glass composition.[13]

The density of the sintered specimens, liquid absorption, and open porosity percentage of them was measured by the Archimedes method using American Society for Testing Material (ASTM) standards.[14,15] It is worth noting that phosphate base glasses were soluble in water, so ethanol and petroleum were used instead of water. The measurements for three pellets were reported as a mean density for each two mentioned liquids and the average of them was calculated.

Scanning Electron Microscope (SEM)/Energy Dispersive X-Ray Analysis (EDX) (VEGA II TESCAN) was employed to investigate the microstructure of the sintered specimens. For this purpose, samples were etched with a mixed acid solution (H_2SO_4 + HCl + H_2O, 1: 3: 2 in volume) and then coated with silver.

2.3 *Solubility and bioactivity of glass-ceramics*

To assess the bioactivity of the sintered specimen, the formation of apatite on the sintered glass-ceramic surfaces was considered, five specimens of each glass composition were considered for this evaluation. The sintered specimens were weighted precisely and then immersed in SBF solution for 3, 5, 7, 14, and 28 days in an incubator (Memmert INB200) at 37 °C.

The SBF solution was prepared using a method described by Kokubo et al.[16] Subsequently, the immersed specimens were removed and gently washed with deionized water and then desiccated at 65 °C for 48 hours. Eventually, dried specimens were weighted for evaluating the weight loss (WL) percentage, during immersing in SBF to determine the dissolution behavior of samples according to the following Eq.:[17]

$$WL(\%) = \frac{W1 - W2}{W1}$$

Where W1 is the sample's weight before immersing and W2 is the weight of desiccated samples after immersing.

pH changes in the solutions were recorded for varied immersing times using the pH meter (BEL PHS3-BW) and compared to a blank sample including only SBF.

The inductively coupled plasma-optical emission spectrometer (Shimadzu ICPS7000) was utilized to specify the variation of Ca ion concentrations in SBF solutions at predetermined immersing periods.

3. Results and discussion

3.1 *Sintering behavior of the glasses*

As was mentioned the compacted samples were sintered at temperatures 570, 600, 615, 635, and 700 °C for 1 h to determine the optimum sintering temperature of glasses. These temperatures extend from the dilatometric softening points of the base glass composition to its crystallization temperature. Glasses sintered at 570 °C didn't have enough strength to measure their sintering parameters. The mean densities, liquid absorption, and presence of open porosity of the specimens after sintering at different temperatures are given in Table 2. As it is observed, the maximum densification has happened at 600 °C for all glasses. It seems that the main reason for this short sintering region of glasses, i.e. 570-600 °C, should be due to bloating of them immediately at temperatures upper than 600 °C. A premature formation of the glass phase on the surface of the specimens and the presence of some elements which are susceptible to exit in the form of gas can be considered as a cause of bloating. Phosphate-based glasses suffer from insufficient chemical resistance and can absorb the moisture of the environment during preparation and storage; so, the absorbed -OH groups are the other

sources for bloating. Based on these explanations, 600 °C was considered as the optimum sintering temperature.

The maximum sintering density at this temperature was obtained for sample 5. It can be attributed to the higher substitution of calcium oxide for strontium and zinc oxides in this glass as well as a higher density of these oxides than calcium one. Glass 3, experienced the minimum percentage of liquid absorption and open porosity at the optimum sintering temperature. It can be concluded that this sample had the best sinterability compared to other compositions.

Table 2. Various parameters of the samples sintered at the indicated temperatures

Samples (code-temperatures/°C)	bulk density (g/cm^3)	liquid absorption (%)	open porosity (%)
1-600	1.69	3.21	6.74
1-615	1.18	7.78	11.48
1-635	1.32	6.34	10.38
1-700	0.89	37.98	42.52
2-600	1.91	2.54	6.01
2-615	1.52	7.74	14.71
2-635	0.94	22.56	26.99
2-700	0.65	38.43	31.38
3-600	2.32	1.04	2.94
3-615	1.64	5.36	14.58
3-635	1.39	10.21	17.82
3-700	0.73	37.49	34.31
4-600	2.23	2.17	6.06
4-615	1.34	9.86	16.51
4-635	1.31	11.11	18.29
4-700	0.95	26.94	32.03
5-600	2.39	1.42	4.19
5-615	1.52	4.83	9.14
5-635	1.17	15.11	22.33
5-700	1.07	18.32	24.37

3.2 *Crystallization behavior*

X-ray diffraction analysis (XRD) patterns of the prepared glass powders are shown in Figure 1. It can be seen that there is not any specific peak in the patterns of glasses 1, 2, and 3, which confirms they are amorphous, while glasses 4 and 5 have started to crystallize. Figure 2 shows the XRD patterns of glasses after sintering at 600°C for 1 h.

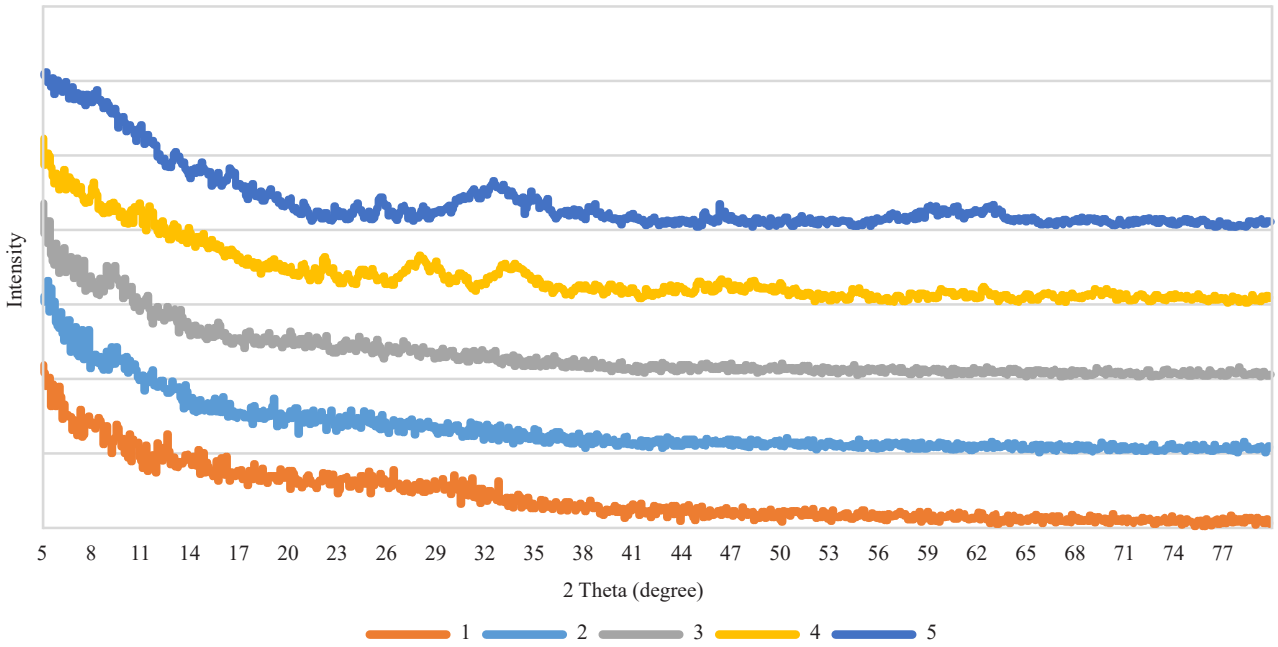

Figure 1. XRD patterns of the glasses

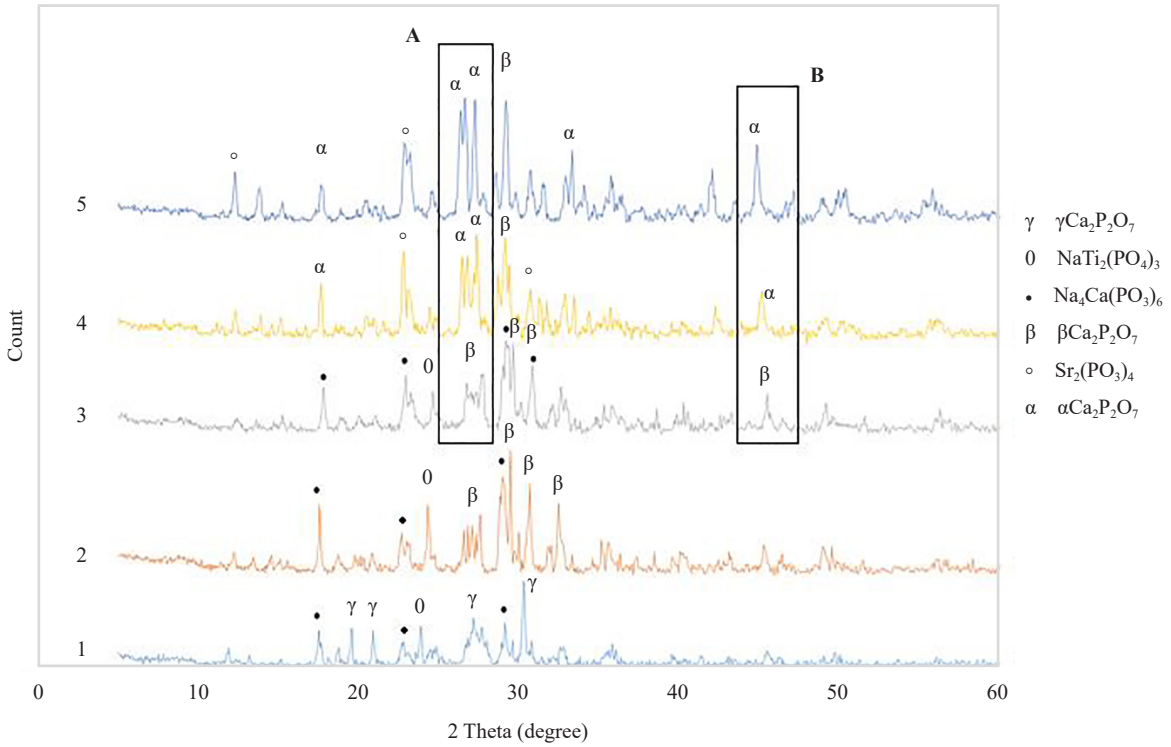

Figure 2. XRD patterns of all glasses sintered at 600 °C for an hour then freely cooled inside the furnace

XRD analysis illustrates that while gamma calcium pyrophosphate ($\gamma Ca_2P_2O_7$) is the major precipitated crystalline phase, sodium-calcium phosphate ($Na_4Ca(PO_3)_6$) and sodium-titanium phosphate ($NaTi_2(PO_4)_3$) are crystallized as minor phases in glass 1. Gamma calcium pyrophosphate transforms into beta form with the tetragonal structure at 700-750 °C.[18] XRD analysis of glass 2, indicates that beta calcium pyrophosphate ($\beta Ca_2P_2O_7$), $Na_4Ca(PO_3)_6$, and $NaTi_2(PO_4)_3$ have been precipitated in it. Substitution of SiO_2 for P_2O_5 can cause phase transformation of gamma calcium pyrophosphate to beta form and stabilizing it at low temperatures.[19]

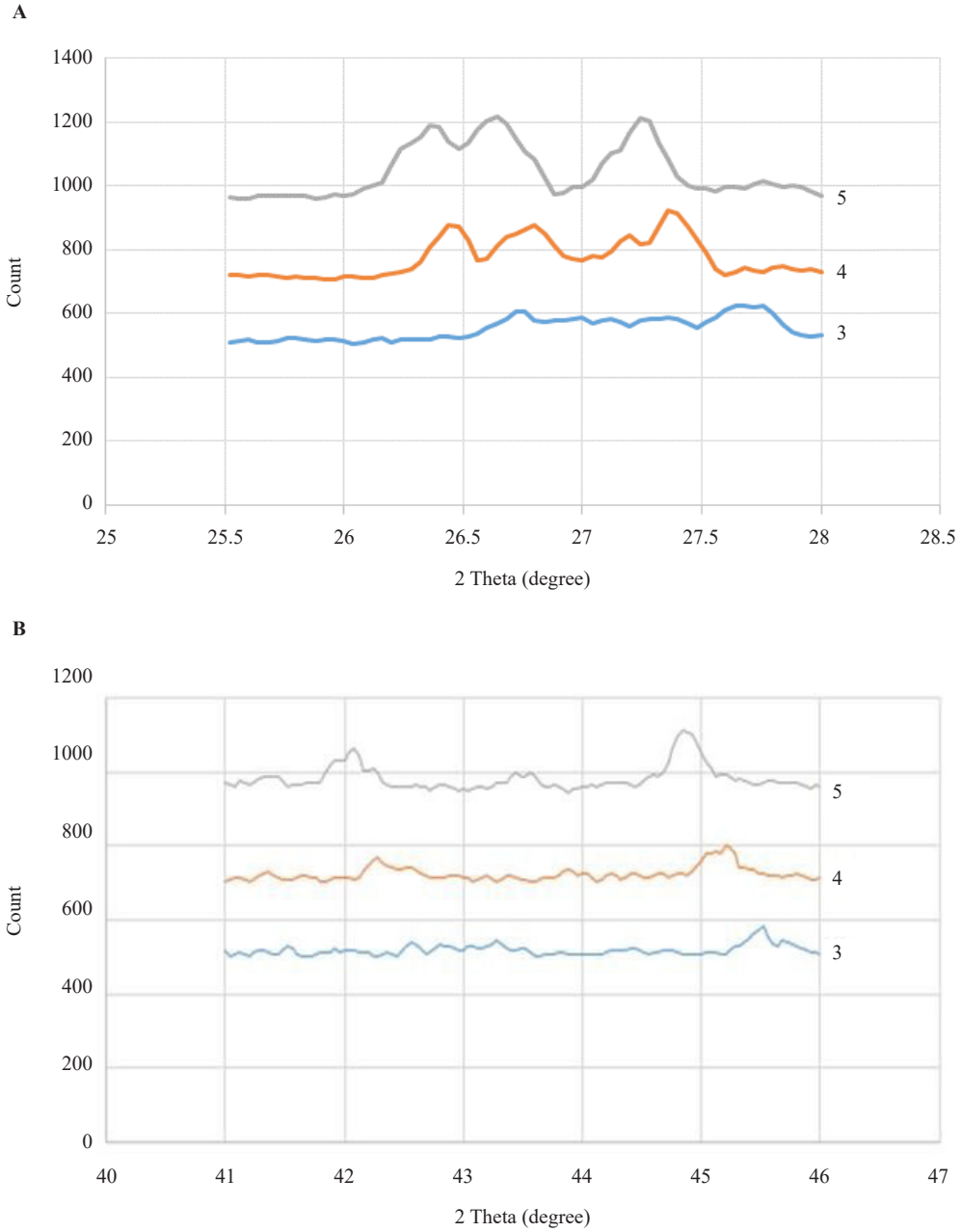

Figure 3. Intensifying and shifting XRD patterns of the major (A) and minor (B) peaks of alpha calcium pyrophosphate with increasing strontium content

XRD pattern of glass 3 illustrates that substituting a low amount of strontium and zinc oxides for calcium oxide has not modified its crystallization behavior and the same crystalline phases have been precipitated in it during heat treatment, However, by increasing the substituted amounts of SrO and ZnO for CaO in glasses 4 and 5, strontium phosphate ($Sr_2(PO_3)_4$) appears as a minor phase. Indeed, strontium can incorporate, instead of calcium, in the same crystalline structure.[20] On the other hand, beta calcium pyrophosphate, a high-temperature form of $\alpha Ca_2P_2O_7$ is also observed as a major phase. Since alpha calcium pyrophosphate has a looser structure than beta form,[21] it could be assumed that the replacement of strontium ions, with a larger ionic radius than calcium, has stabilized the beta one at room temperature. Based on the Bragg equation ($n\lambda = 2d\sin\theta$) diffraction patterns should be shifted to lower angles by strontium substitution. It can be seen that in the strontium containing samples the major (Figure 3A) and minor (Figure 3B) peaks of alpha calcium pyrophosphate have intensified and shifted considerably to lower 2-theta with increasing strontium content.

3.3 *Scanning electron microscope investigations*

SEM micrographs of the samples sintered at 600 °C for one hour are given in Figure 4. It has been reported that gamma and beta forms of calcium pyrophosphate have plate-like morphologies;[7,8,10,22] hence, the plate-like phases in these SEM micrographs can be attributed to these phases. On the other hand, it is said that sodium titanium phosphate tends to be agglomerated and its morphology is irregular;[23] the phase which has been pointed with the yellow arrow (Figure 4B) can be attributed to this phase, based on the EDX analysis. Accordingly, samples 1, 2, and 3 which contain similar crystalline phases show almost similar SEM micrographs (Figure 4A-C). The rod-like particles in these microstructures are probably the immature calcium pyrophosphates, which their growth would ultimately lead to the plate-like ones.

One can observe three different morphologies such as plate-like, needle-like, and granular-like in sample 5 (Figure 4E). Since beta calcium pyrophosphate has a plate-like morphology (green arrow shows it) the two other morphologies in this micrograph could be attributed to alpha calcium pyrophosphate and strontium phosphate. Samples 4 and 5 have similar crystalline phases; therefore, it is expected to have similar microstructures. The plate-like and needle-like particles in the SEM micrograph of sample 4 are attributed to alpha calcium pyrophosphate and strontium phosphate, respectively (Figure 4D).

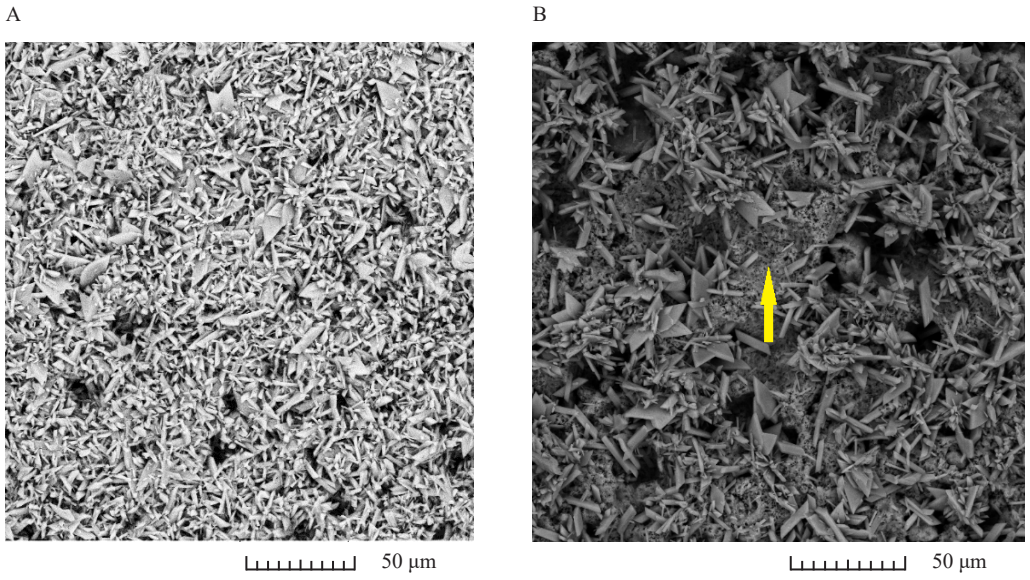

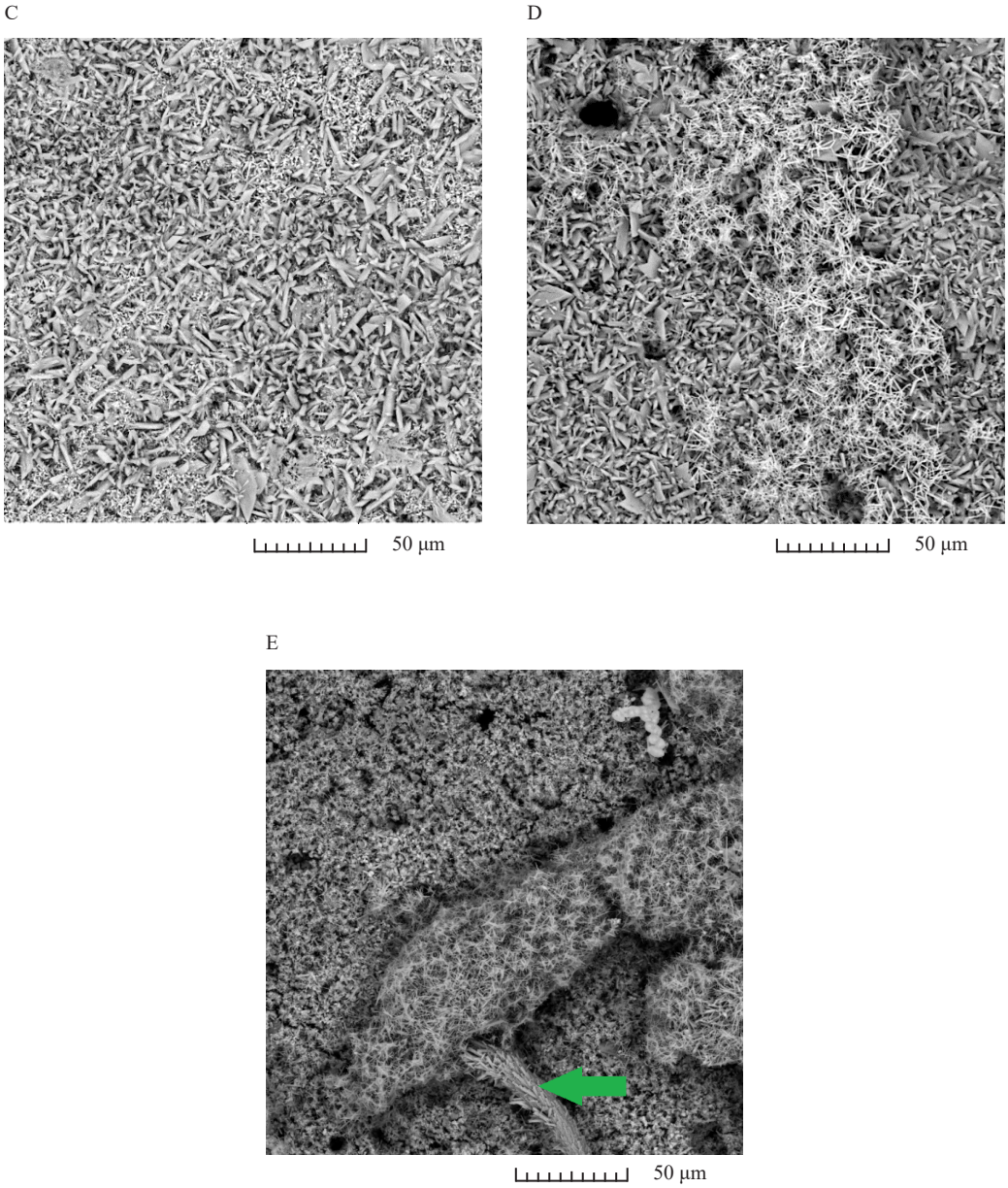

Figure 4. SEM micrographs of glass-ceramic samples sintered at 600 °C for 1 h, then freely cooled inside the furnace after etching, at magnification × 1000, A-E for sample 1-5, respectively

3.4 *Dissolution behavior of glass-ceramics in SBF*

To evaluate the dissolution behavior of the glass-ceramics in the body, the chemical durability of both amorphous and crystallized samples was considered. Weight loss percentage of the samples after immersing in SBF solution was considered as a criterion for this property, which is shown in Figure 5 for the samples sintered at 600 °C as a function of immersion time.

It is said that the dissolution of phosphate-based glasses in aqueous solutions occurs in two steps:

1) Hydration reaction means the formation of a hydrated layer on the surface of glass due to the interchanging of H^+ ion from the solution with Na^+ ion from the glass at the medium-glass interface;

2) Network breakage means that the P-O-P bonds break during the hydrolysis of phosphate glass which brings about the destruction of the polymeric phosphate network.[24]

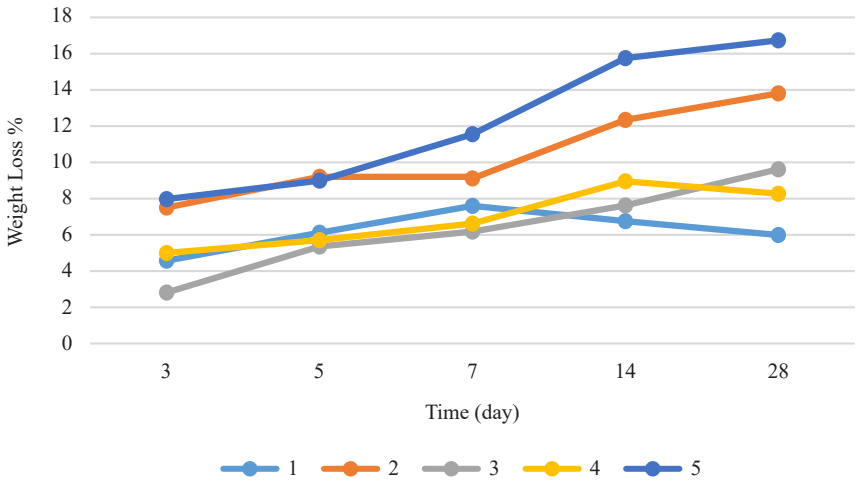

Figure 5. Weight loss of the samples as a function of incubation time

In general, the weight loss percentage of all samples have slightly increased with the incubation time. Also, glass 3 has experienced the least weight loss, compared to other samples in the first week of incubation. It can be attributed to the less open porosity and liquid absorption percentages of this sample. On the other hand, the least weight loss of glass 1 at the end of incubation time could be attributed to the presence of gamma calcium pyrophosphate which has high chemical durability.[25] The weight loss percentages of glass 5 has increased just before 5 days of incubation. Moreover, this sample experienced the most weight loss during soaking in SBF compare with the other samples. As it has almost the least liquid absorption, one can attribute its low chemical resistance to its high amounts of strontium. The larger atomic radius of strontium compared to calcium makes it more susceptible to hydrolysis.[26] Furthermore, the atomic bond of strontium can be weaker than calcium since its electronegativity is less than calcium.

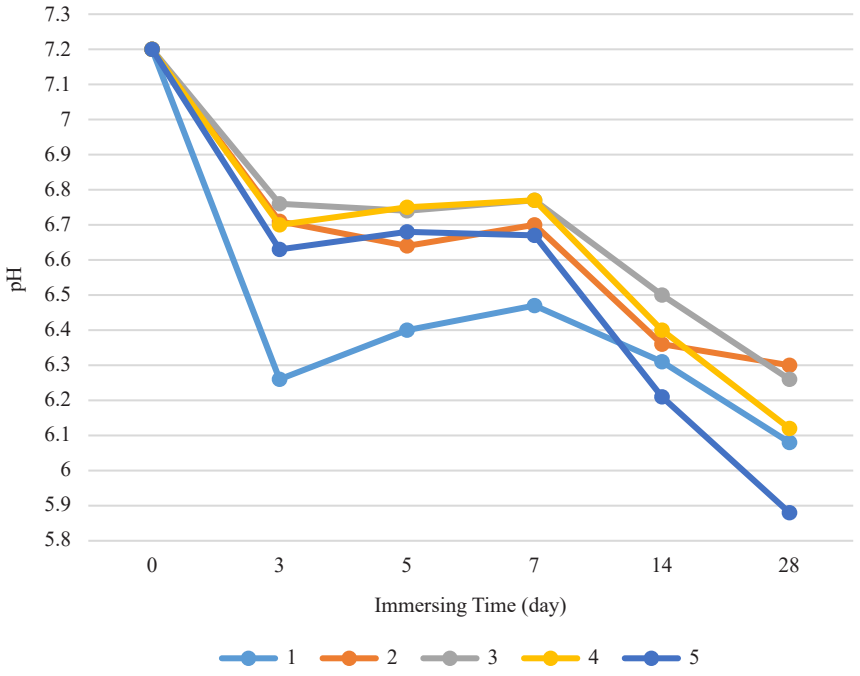

Figure 6. pH variation in the SBF solution as a function of immersing time

pH variation in the SBF solution as a function of immersing time is given in Figure 6. This can be explained by ion dissolution from the surface of glass-ceramic and subsequent composition changes.

As can be seen in Figure 6, all samples experienced a considerable decrease in the pH during the first 3 days of incubation. It may be related to phosphate ions release and phosphoric acid formation due to glass dissolution.[27] Its subsequent increase is due to decreasing the concentration of H^+ ions in the medium which can be attributed to cations substitution or releasing and following OH^- ion generation.[24,28] Cation releasing from the glass due to glass destruction leads to change its charge balance. So, H^+ can migrate to the glass from the solution and this may result in a pH increase.[29] Besides, all samples experienced a second decrease in the pH of the solution after 7 days. This can be due to the leaching of the amorphous matrix of glass-ceramics which could confirm a layer by layer glass dissolution.[24] In other words, releasing the rate of phosphate ions from the glass could be higher than the cation releasing rate after the seventh day of soaking.

Since glass 5 experienced the maximum weight loss compared to the other samples at the end of incubation, it could be expected that its pH would be lower than others.

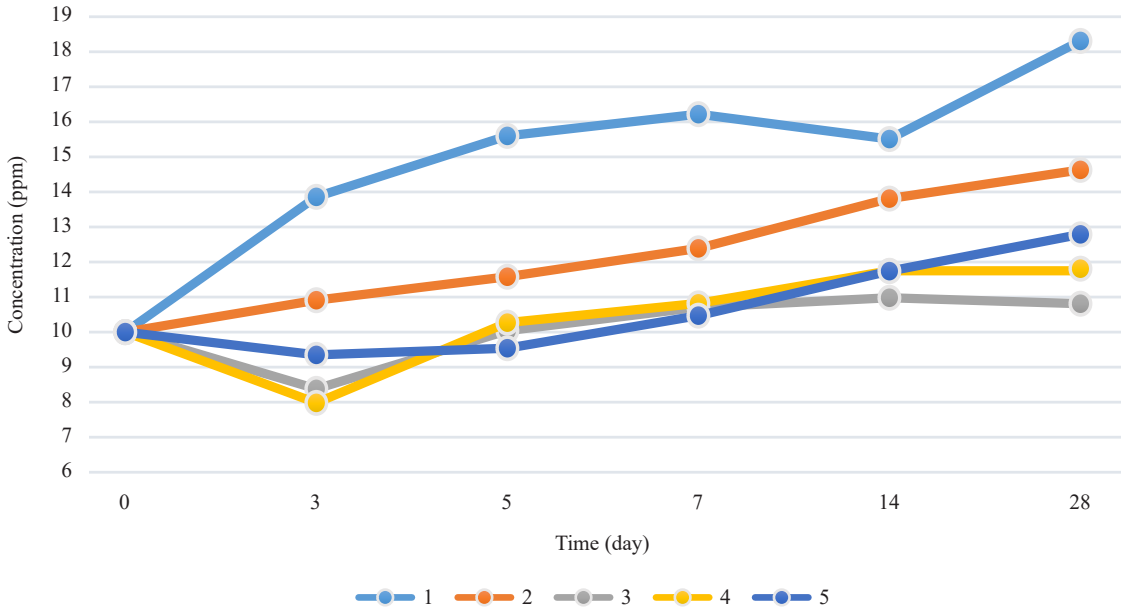

Figure 7. Cumulative release of Ca^{2+} as a function of immersing time

The cumulative release of Ca^{2+} as a function of soaking time for the resulted samples is reported in Figure 7. Samples that do not contain strontium and zinc released calcium up to day 5, which could be attributed to the dissolution of glass-ceramics. On the other hand, strontium and zinc-containing samples experienced a decrease in the concentration of Ca^{2+} in the first five days of incubation. It can be because of apatite-like layer formation on the surface of these samples which consumed Ca^{2+} ions from the SBF solution.[14,15] However, Ca^{2+} concentration rose slightly after 5 days which maybe because of the destruction of the top layer and then the exposure of a fresh one. It can be expected that since samples 1 and 2 have higher calcium contents, their cumulative release of Ca^{2+} should be higher than others.

3.5 *SEM observation of immersed specimens in SBF*

To evaluate the bioactivity and hydroxyapatite formation ability of glass-ceramics in SBF, the surface of all samples before and after immersing in SBF for 3 and 28 days, were investigated. Figure 8 depicts the obtained results.

As is observed, apatite-like agglomerates deposited on the surface of the sample after three days of immersing in the SBF solution (Figure 8B). But, at the end of immersing time, they have dissolved in the solution due to the destruction of the specimen.

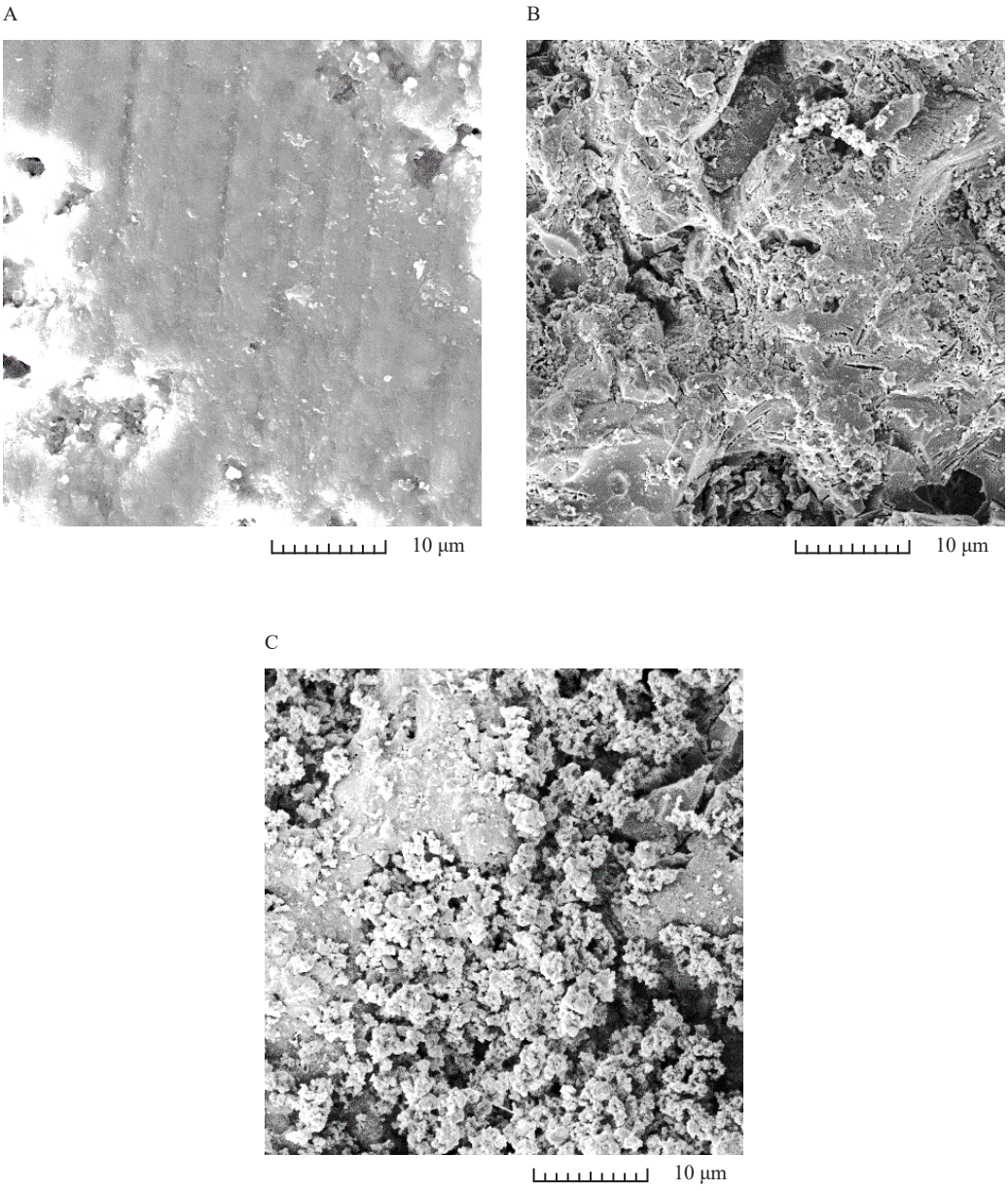

Figure 8. SEM micrographs of sample 1 before (A) and after immersing in SBF solution for 3 days (B) and 28 days (C) at magnification × 5000

Increasing the cumulative release of Ca^{2+} and decreasing the pH of the solution can confirm the destruction of the substrate and a layer by layer dissolution mechanism which brings about the dissolution of deposited apatite-like agglomerates. On the other hand, some residues of apatite-like agglomerates can be seen on the surface of the sample at the end of immersing time (Figure 8C). Since sample 1 experienced the least weight loss percentage compare to the other samples, they can be attributed to the residual apatite agglomerates on the surface of the gamma calcium pyrophosphate phase. Otherwise, they can be the fresh ones deposited on the new surface layer of the sample. Similar

trends for samples 2 and 3 were observed too. By day 3 apatite-like agglomerates precipitated on the surface of samples (Figure 9B and Figure 10B respectively). But, after four weeks of immersing most of them were leached by the substrate dissolution (Figure 9 and Figure 10C respectively). Since sample 4 has experienced the least cumulative calcium ion release from day 0 through day 5 it can be related to the calcium consumption from the solution leading to the apatite-like layer formation on its surface (Figure 11A).[30] Also, as its weight-loss percentage and pH decrease were relatively lower than the other samples over 4 weeks, it can be concluded that sample 4 has experienced a moderate dissolution rate. Consequently, aggregated apatite-like agglomerates can be expected to be observed on the surface of the sample at the end of the immersing period (Figure 11C).

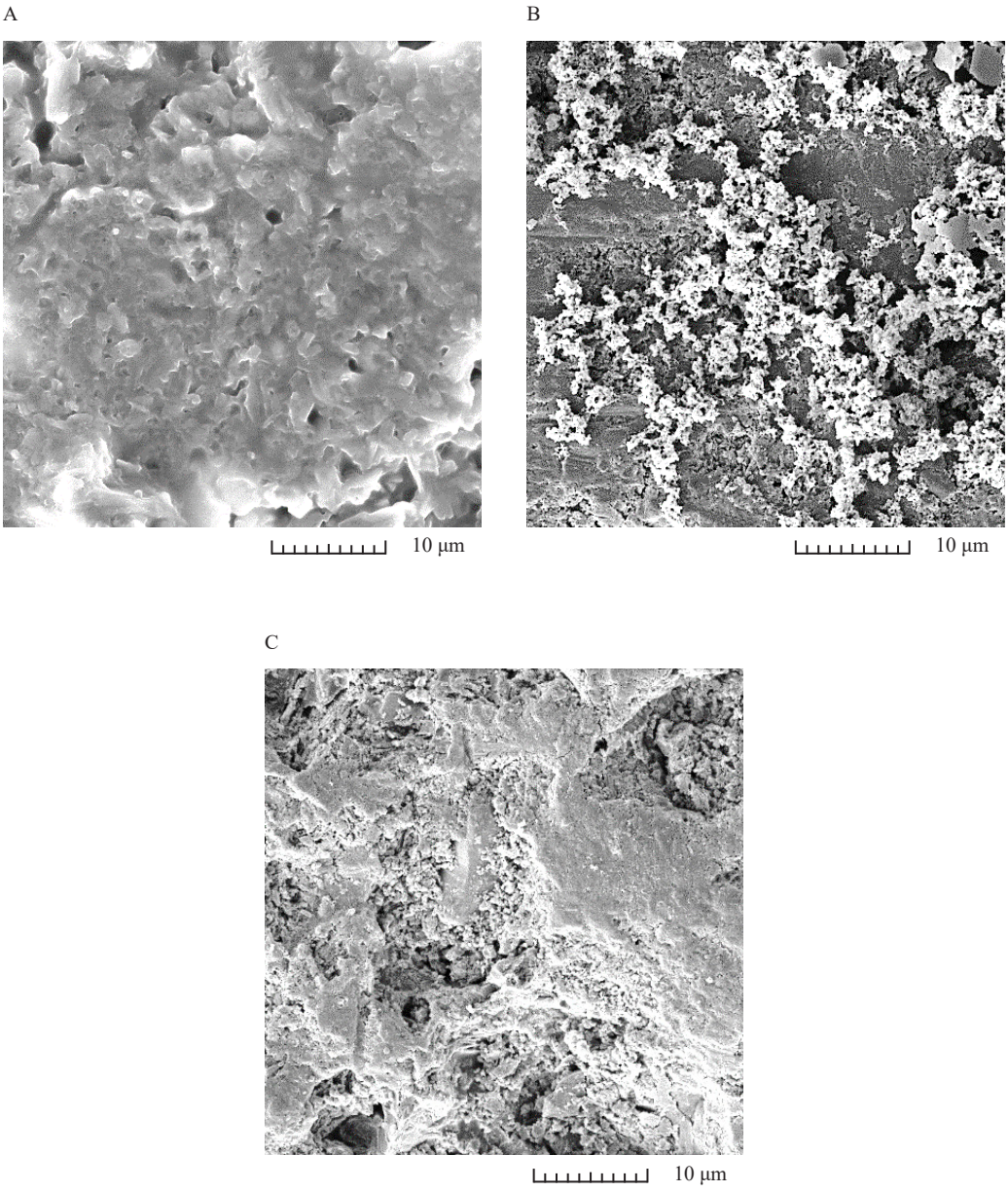

Figure 9. SEM micrographs of sample 2 before (A) and after immersing in SBF solution for 3 days (B) and 28 days (C) at magnification × 5000

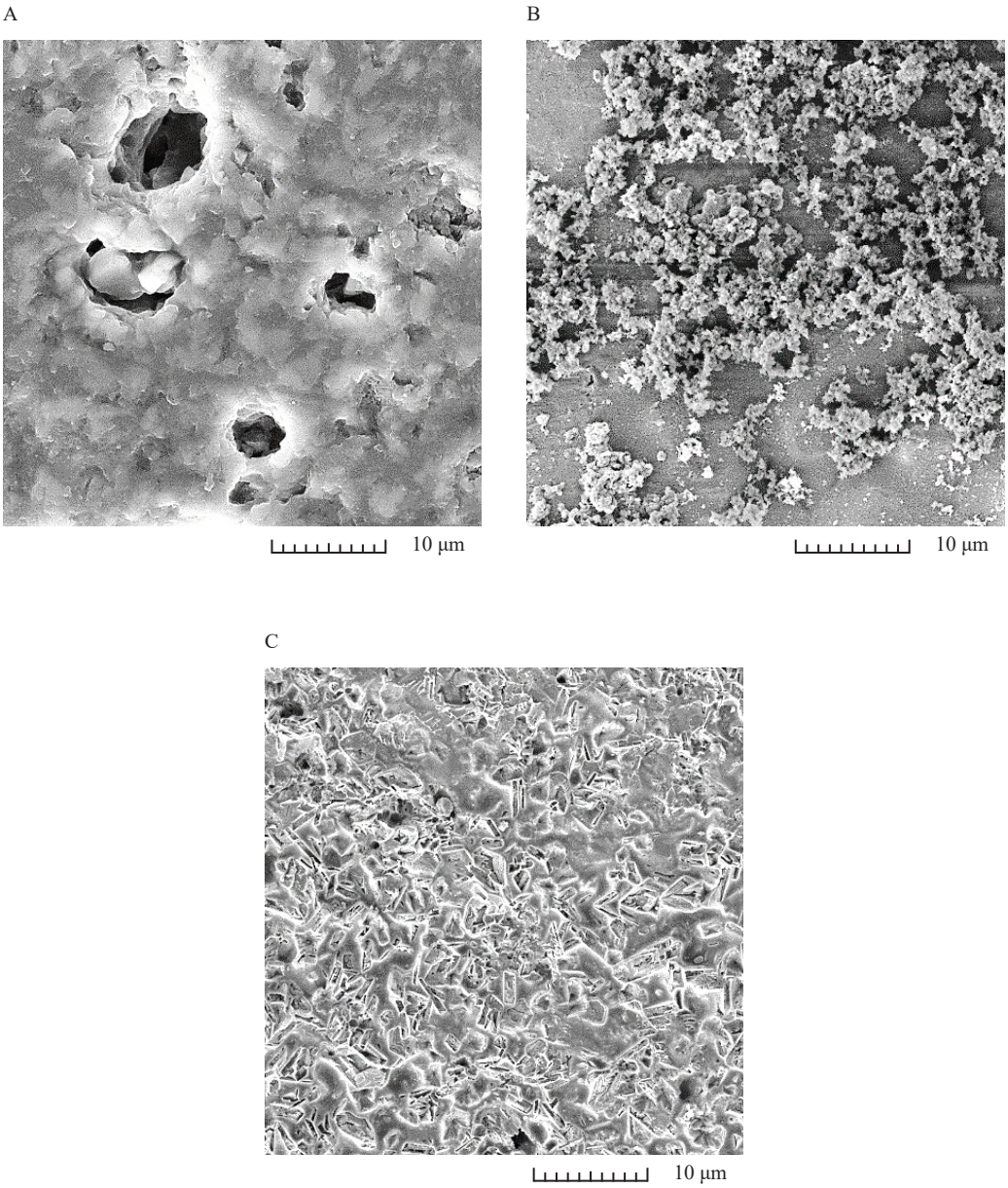

Figure 10. SEM micrographs of sample 3 before (A) and after immersing in the SBF solution for 3 days (B) and 28 days (C) at magnification × 5000

SEM micrographs of sample 5 demonstrated that like the other samples, agglomerates of hydroxyapatite were deposited on the surface of the sample by day 3 (Figure 12B). But, they dissolved in the solution due to the substrate dissolution at the end of the immersing period (Figure 12C). The weight-loss percentage and pH changes of this sample confirm a high dissolution rate, which can be in agreement with the high activity of this sample that causes a new hydroxyapatite formation on the fresh surface layer (Figure 12C).

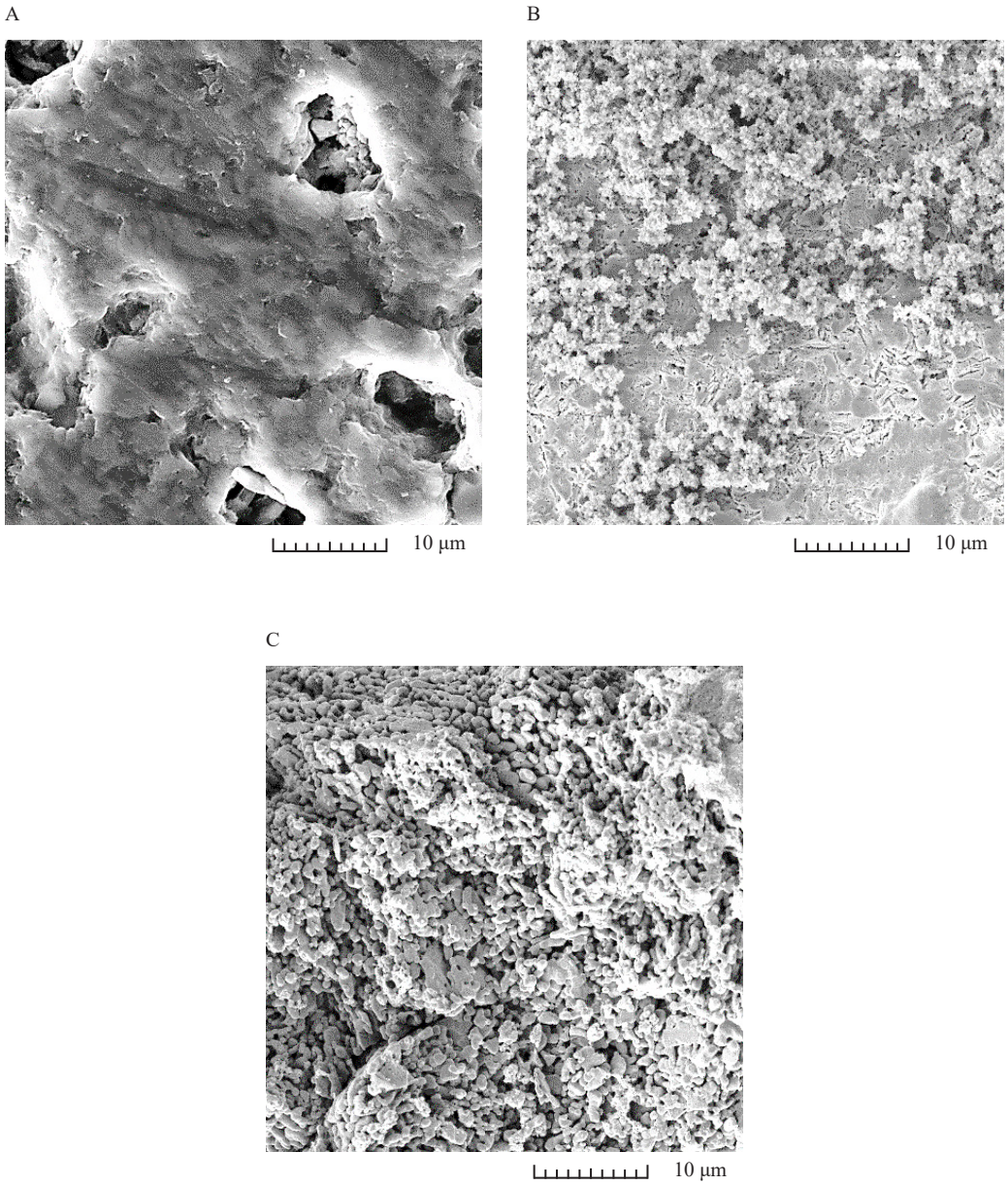

Figure 11. SEM micrographs of sample 4 before (A) and after immersing in SBF solution for 3 days (B) and 28 days (C) at magnification × 5000

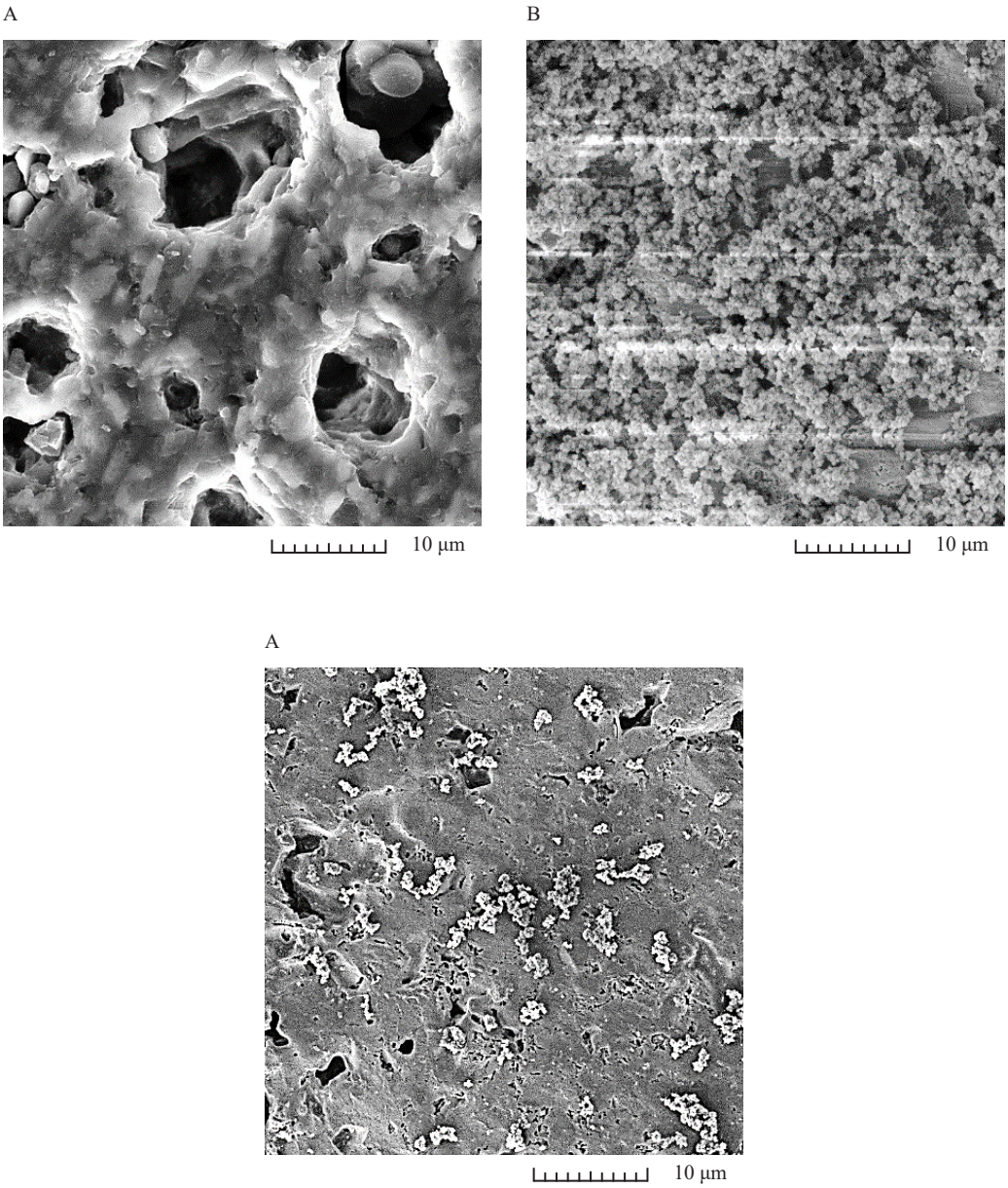

Figure 12. SEM micrographs of sample 5 before (A) and after immersing in SBF solution for 3 days (B) and 28 days (C) at magnification × 5000

4. Conclusion

The melt quench technique was applied to synthesize phosphate based glass-ceramics in the system of P_2O_5-CaO-Na_2O-TiO_2 with various substitution amounts of SrO and ZnO for CaO. Sinterability, crystallization, dissolution behavior, and bioactivity of glass-ceramics were evaluated. 600 °C was designated as the optimum sinter temperature. While, the substitution of 3.05 and 0.305 mol% of strontium and zinc oxides for CaO in glass 3, leads to its best sinterability compare to the other compositions. Calcium pyrophosphate was determined as the main crystalline phase for all samples, which transformed from gamma to beta by SiO_2 substitution. On the other hand, Strontium substitution can stabilize the high-temperature form of calcium pyrophosphate (alpha). It is noteworthy to point out that a low amount of zinc oxide leads to its absence in the crystalline phase of glass-ceramics. The dissolution rate of glass-ceramics increased with the substitution of strontium and zinc oxides. Apatite-like agglomerates were deposited on the

surfaces of all samples at the first stage of incubation in the SBF solution. But, they were destructed by the substrate dissolution. However, some residues of the grown apatite-like layer were observed on the surface of Sample 4. It can be concluded that substitution of 7.62 and 0.76 mol% of SrO and ZnO respectively, can cause maintaining apatite-like layer due to the dissolution rate controlling.

Conflict of interest

The authors declare no competing financial interest.

References

[1] Courthéoux, L.; Lao, J.; Nedelec, J. M.; Jallot, E. Controlled Bioactivity in Zn-doped Sol-Gel Derived SiO2-CaO Bioactive Glasses. *J. Phys. Chem. C, Am. Chem. Soc*. **2008,** *112*(35), 13663-13667.

[2] El-Kady, A. M.; Ali, A. F. Fabrication and Characterization of ZnO Modified Bioactive Glass Nanoparticles. *Ceram. Int*. **2012,** *38*(2), 1195-1204.

[3] Reginster, J. Y.; Felsenberg, D.; Boonen, S.; Diez-Pere, A. O.; Rizzoli, R.; Brandi, M. L.; Spector, T. D.; Cormier, C.; Balogh, A.; Delmas, P. D.; Meunier, P. J. Effects of Long-Term Strontium Ranelate Treatment on the Risk of Nonvertebral and Vertebral Fractures in Postmenopausal Osteoporosis: Results of a Five-Year, Randomized, Placebo-Controlled Trial. *Arthritis Rheum*. **2008,** *58*(6), 1687-1695.

[4] Meunier, P. J.; Roux, C.; Seeman, E.; Ortolani, S.; Badurski, J. E.; Spector, T. D.; Cannata, J.; Balogh, A.; Lemmel, E. M.; Nielsen, S. P.; Rizzoli, R.; Genant, H. K.; Reginster, J. Y. The Effects of Strontium Ranelate on the Risk of Vertebral Fracture in Women with Postmenopausal Osteoporosis. *N. Engl. J. Med.* **2004,** *350*(5), 459-468.

[5] Gentleman, E.; Fredholm, Y. C.; Jell, G.; Lotfibakhshaiesh, N.; O'Donnell, M. D.; Hill, R. G.; Stevens, M. M. The effects of strontium-substituted bioactive glasses on osteoblasts and osteoclasts in vitro. *Biomaterials*. **2010,** *31*, 3949-3956.

[6] Xiang, Y.; Du, J.; Skinner, L. B.; Benmore, C. J.; Wren, A. W.; Boyd, D. J.; Towler, M. R. Structure and diffusion of ZnO-SrO-CaO-Na_2O-SiO_2 bioactive glasses: A combined high energy X-ray diffraction and molecular dynamics simulations study. *RSC Adv*. **2013,** *3*(17), 5966-5978.

[7] Rezaei, Y.; Moztarzadeh, F., Shahabi, S.; Tahriri, M. Synthesis, Characterization, and in Vitro Bioactivity of Sol-Gel-Derived SiO_2-CaO-P_2O_5-MgO-SrO Bioactive Glass, Synthesis and Reactivity in Inorganic. *Metal-Organic, and Nano-Metal Chem*. **2014,** *44*(5), 692-701.

[8] Fredholm, Y. C.; Karpukhina, N.; Brauer, D. S.; Jones, J. R.; Law, R. V.; Hill, R. G. Influence of Strontium for Calcium Substitution in Bioactive Glasses on Degradation, Ion Release and Apatite Formation. *J. R. Soc. Interface*. **2012,** *9*(70), 880-889.

[9] Wu, C.; Zhou, Y.; Lin, C.; Chang, J.; Xiao, Y. Strontium-Containing Mesoporous Bioactive Glass Scaffolds with Improved Osteogenic/Cementogenic Differentiation of Periodontal Ligament Cells for Periodontal Tissue Engineering. *Acta Biomater*. **2012,** *8*(10), 3805-3815.

[10] Wu, X.; Meng, G.; Wang, S.; Wu, F.; Huang, W.; Gu, Z. Zn and Sr Incorporated 64S Bioglasses: Material Characterization, in-vitro Bioactivity and Mesenchymal Stem Cell Responses. *Mater. Sci. Eng. C*. **2015,** *52*, 242-250.

[11] Murphy, S.; Wren, A. W.; Towler, M. R.; Boyd, D. The effect of ionic dissolution products of Ca-Sr-Na-Zn-Si Bioactive Glass on in Vitro Cytocompatibility. *J. Mater. Sci. Mater. Med.* **2010,** *21*(10), 2827-2834.

[12] Boyd, D.; Carroll, G.; Towler, M. R.; Freeman, C.; Farthing, P.; Brook, I. M. Preliminary Investigation of Novel Bone Graft Substitutes Based on Strontium-Calcium-Zinc-Silicate Glasses. *J. Mater. Sci. Mater. Med.* **2009,** *20*(1), 413-420.

[13] Khorasanizadeh, F.; Eftekhari, Y. B.; Safaei-Naeini, Y. Crystallization and Sinterability behaviour of Bioresorbable CaO-P_2O_5-Na_2O-TiO_2 Glass Ceramics for Bone Regeneration Application. *Iranian Journal of Materials Science & Engineering*. **2013,** *10*(1), 18-27.

[14] Standard Test Methods for Apparent Porosity, Liquid Absorption , Apparent Specific Gravity, and Bulk Density of Refractory Shapes by Vacuum Pressure. https://www.astm.org/c0830-00.html (accessed July 5, 2019).

[15] Standard Test Methods for Density of Compacted or Sintered Powder Metallurgy (PM) Products Using Archimedes' Principle1. https://tajhizkala.ir/doc/ASTM/B962.pdf (accessed July 24, 2019).

[16] Kokubo, T.; Takadama, H. How Useful is SBF in Predicting in Vivo Bone Bioactivity? *Biomaterials*. **2006,** *27*(15), 2907-2915.
[17] Vaz, C. M.; Fossen, M.; van Tuil, R. F.; de Graaf, L. A.; Reis, R. L.; Cunha, A. M. Casein and soybean protein-based thermoplastics and composites as alternative biodegradable polymers for biomedical applications. *J. biomed. mat. research, Part A*. **2003,** *65*(1), 60-70.
[18] Bian, J. J.; Kim, D. W.; Hong, K. S. Phase transformation and sintering behavior of $Ca_2P_2O_7$. *Mat. Lett*. **2004,** *58*(3-4), 347-351.
[19] Ming, C. Q.; Greish, Y.; El-Ghannam, A. Crystallization behavior of silica-calcium phosphate biocomposites: XRD and FTIR studies. *J. Mat. Sci. Materials in Medicine.* **2004,** *15*(11), 1227-1235.
[20] Massera, J.; Mayran, M.; Rocherullé, J.; Hupa, L. Crystallization behavior of phosphate glasses and its impact on the glasses' bioactivity. *J. Mat. Sci.* **2015,** *50*(8), 3091-3102.
[21] Bian, J.; Kim, D. W.; Hong, K. Microwave dielectric properties of $(Ca_{1-x}Zn_x)_2P_2O_7$. *Mat. Lett*. **2005,** *59*(2-3), 257-260.
[22] Safronova, T. V.; Putlyaev, V. I.; Kurbatova, S. A.; Shatalova, T. B.; Larionov, D. S.; Kozlov, D. A.; Evdokimov, P. V. Properties of amorphous calcium pyrophosphate powder synthesized via ion exchange for the preparation of bioceramics. *Inorg. Mat*. **2015,** *51*(11), 1177-1184.
[23] Sun, F.; Wang, R.; Jiang, H.; Zhou, W. Synthesis of sodium titanium phosphate at ultra-low temperature. *Res. Chem. Intermed*. **2013,** *39*(4), 1857-1864.
[24] Majhi, M. R.; Pyare, R.; Singh, S. P. Studies on Preparation and Characterization of Na_2O-CaO-P_2O_5-ZrO_2 Bioglass-ceramics. *Inter. J. of Scientific & Eng. Research*. **2011,** *2*(8), 1-13.
[25] Radev, L.; Zheleva, D.; Michailova, I. In vitro bioactivity of Polyurethane/85S Bioglass composite scaffolds. *Open Chem*. **2013,** *11*(9), 1439-1446.
[26] Al Qaysi, M.; Walters, N. J.; Foroutan, F.; Owens, G. J.; Kim, H. W.; Shah, R.; Knowles, J. C. Strontium-and calcium-containing, titanium-stabilised phosphate-based glasses with prolonged degradation for orthopaedic tissue engineering. *J. Biomaterials Appl*. **2015,** *30*(3), 300-310.
[27] Lakhkar, N. J.; Abou Neel, E. A.; Salih, V.; Knowles, J. C. Strontium oxide doped quaternary glasses: Effect on structure, degradation and cytocompatibility. *J. Mat. Sci. Materials in Medicine*. **2009,** *20*(6), 1339-1346.
[28] Rajkumar, G.; Rajkumar, M.; Rajendran, V.; Aravindan, S. Influence of Ag_2O in physico-chemical properties and HAp precipitation on phosphate-based glasses. *J. Am. Ceram. Soc.* **2011,** *94*(9), 2918-2925.
[29] Massera, J.; Petit, L.; Cardinal, T.; Videau, J. J.; Hupa, M.; Hupa, L. Thermal properties and surface reactivity in simulated body fluid of new strontium ion-containing phosphate glasses. *J. Mat. Sci. Materials in Medicine*. **2013,** *24*(6), 1407-1416.
[30] Shu, C.; Wenjuan, Z.; Xu, G.; Wei, Z.; Wei, J.; Dongmei, W. Issolution behavior and bioactivity study of glass ceramic scaffolds in the system of CaO-P_2O_5-Na_2O-ZnO prepared by sol-gel technique. *Mat. Sci. Eng. C*. **2010,** *30*, 105-111.